IEEE Access
Multidisciplinary | Rapid Review | Open Access Journal

Received October 15, 2020, accepted November 13, 2020, date of publication November 17, 2020,
date of current version December 2, 2020.

Digital Object Identifier 10.1109/ACCESS.2020.3038817

A Systematic Review of Breast Cancer Detection Using Thermography and Neural Networks

MOHAMMED ABDULLA SALIM AL HUSAINI[1], MOHAMED HADI HABAEBI[1], (Senior Member, IEEE), SHIHAB A. HAMEED[2], (Senior Member, IEEE), MD. RAFIQUL ISLAM[1], (Senior Member, IEEE), AND TEDDY SURYA GUNAWAN[1], (Member, IEEE)

[1]Department of Electrical Computer Engineering, International Islamic University Malaysia, Kuala Lumpur 50728, Malaysia
[2]Department of Computer Science, Cihan University-Erbil, Erbil 8415683111, Iraq

Corresponding author: Mohamed Hadi Habaebi (habaebi@iium.edu.my)

This work was supported in part by the IoT and Wireless Communications Laboratory, and in part by IIUM Publication under Grant P-RIGS18-003-0003.

ABSTRACT Breast cancer plays a significant role in affecting female mortality. Researchers are actively seeking to develop early detection methods of breast cancer. Several technologies contributed to the reduction in mortality rate from this disease, but early detection contributes most to preventing disease spread, breast amputation and death. Thermography is a promising technology for early diagnosis where thermal cameras employed are of high resolution and sensitivity. The combination of Artificial Intelligence (AI) with thermal images is an effective tool to detect early stage breast cancer and is foreseen to provide impressive predictability levels. This paper reviews systematically the related works employing thermography with AI highlighting their contributions and drawbacks and proposing open issues for research. Several different types of Artificial Neural Networks (ANNs) and deep learning models were used in the literature to process thermographic images of breast cancer, such as Radial Basis Function Network (RBFN), K-Nearest Neighbors (KNN), Probability Neural Network (PNN), Support Vector Machine (SVM), ResNet50, SeResNet50, V Net, Bayes Net, Convolutional Neural Networks (CNN), Convolutional and DeConvolutional Neural Networks (C-DCNN), VGG-16, Hybrid (ResNet-50 and V-Net), ResNet101, DenseNet and InceptionV3. Previous studies were found limited to varying the numbers of thermal images used mostly from DMR-IR database. In addition, analysis of the literature indicate that several factors do affect the performance of the Neural Network used, such as Database, optimization method, Network model and extracted features. However, due to small sample size used, most of the studies achieved a classification accuracy of 80% to 100%.

INDEX TERMS Artificial intelligent, breast cancer, thermal camera, deep convolutional neural network.

I. INTRODUCTION

A. HISTORY OF BREAST CANCER DETECTION

Egyptians identified breast cancer 3,000 BC [1]. Then the Greeks, when a woman brought to Hippocrates, had a bloody discharge from the nipple and died. Hippocrates linked breast cancer due to menopause and called it hidden cancer because it did not appear on the skin. In 450 BC, Hippocrates diagnosed the hidden diseases of the patient by placing the mud on the entire body of the patient and the area that first dries out is the disease. It is the primitive process of thermal detection in the medical field [2]. Signs of breast cancer appear bitter in the mouth, loss of appetite, disturbed intelligence, dry eyes and nostrils, and loss of smell [3]. In the first century AD, the surgeon from the school of Alexandria pointed out that breast cancer is a huge swelling of harsh texture and uneven and grey to red.

In 1913, radiography of breast cancer patients began in Germany. The study was carried out on 3,000 patients by surgeon Salmon [4]. In 1951 ultrasound was used as a research tool to detect breast tumor and identify it as benign or malignant. The other research supported in 1952, when 21 cases of breast cancer were successfully identified. Through the results of this research, ultrasound was tested in the hospital as a diagnostic tool for breast cancer in 1954. In the 1960s, improvements made to the internal structure of the ultrasound

The associate editor coordinating the review of this manuscript and approving it for publication was Jenny Mahoney.

system and improvements in detection methods, including placing breasts on controlled temperature water for early detection of the tumor. Technological revolution after 1980 contributed to changes in the detection of the tumor and the flow of blood to the tumor. In the late 20th century it was developed to use ultrasound to guide the needle biopsy in the breast area [5].

In 1957, Lawson used the thermal camera for the first time to diagnose breast cancer when he found the temperature difference of the tumor and the surrounding healthy area. When doctors and surgeons found Lausanne and Ghatmati in 1963 when they published research that the increase in skin temperature associated with breast cancer was associated with venous convection. In 1982, the Food and Drug Administration (FDA) approved the use of a thermal camera as a diagnostic aid to detect breast cancer. In 1996, a comparison between thermal images and X-rays for the diagnosis of a patient was conducted where the disease was detected by the thermal images disease, while it was not detected by X-rays [2].

B. TYPES OF BREAST CANCER IMAGING

1) MAMMOGRAM

Mammograms are the gold standard for breast cancer screening since 1960. However, there are many challenges affecting diagnosis using mammograms such as age, breast tissue density and family history [6]. Mammograms can detect breast cancer in early stage, reducing mortality by 25%. The doses of mammograms used in diagnosis affect patients over 70 years of age and cause rupture of weak tissue in the breast. They may also cause the formation of cancer in these vessels. Also, it is unable to detect cancer in younger women because of the density of breast tissue [7].

2) COMPUTERIZED TOMOGRAPHY (CT)

Computerized tomography takes X-rays of the breast from different angles as the patient enters in a closed machine, and a computer collects the image of the breast. The patient is injected into the vein of his hand with a substance to increase the contrast of the image [8]. Modern image reconstruction techniques have reduced 70% of the radiation and reduced the time it takes to take pictures [9]. However, there are disadvantages to this technique, including that some patients cannot hold breathing. This is in addition to the risk of radiation to the patient and its effect on pregnant women.

3) MAGNETIC RESONANCE IMAGING (MRI)

MRI is a medical examination tool that uses radio waves and a field Magnetic. To show the tumor and calcifications clearly, the patient is injected with a substance into the bloodstream. MRI is often used to follow the response to chemotherapy for breast cancer patients before resorting to breast amputation [10]. Furthermore, when using MRI, the patient must be injected with gadolinium to show the details of the blood vessels in the breast. The syringe Gadolinium has the least effect on the sensitivity of iodine used in X-ray. However, the Gadolinium affects allergic patients, so a supervision doctor is needed.MRI has many disadvantages such as its inability to detect breast cancer at an early stage and it is expensive too. Furthermore, women are not allowed to breast-feed for 48 hours. The device is also a closed space that causes anxiety in claustrophobic patients who are afraid of confined places.

4) ULTRASOUND

Ultrasound imaging based on echo or reflection of sound waves is considered safer and more effective than X-rays. Ultrasound was first used in 1940 by France and Germany in the medical field. Ultrasound can detect breast cancer successfully in women with dense tissue and it has no impact on health and is quick and comfortable [10]. However, the disadvantage of this technique is its inability to detect breast cancer at an early stage and it has a higher rate of false-positive results [77].

5) HISTOLOGY IMAGING

Histological images are generated using a microscope and they allow for the study of the microanatomy of cells, tissues, and organs by examining the correlation between structure and function. To detect cancer, breast tissue is stained with hematoxylin and eosin. The diagnosis of breast cancer histology images with hematoxylin and eosin stained, however, is non-trivial, labor-intensive and often leads to a disagreement between pathologists [15]. Furthermore, the process of generating the images themselves require a microscope that is expensive to acquire and maintain.

C. MOTIVATION FOR AUTOMATED DIAGNOSTIC SYSTEMS

The need for automated diagnostic systems to detect breast cancer rose due to the high percentage of human errors in assessing and detecting breast cancer [52]. In addition, the automated diagnostic system detects breast cancer at a very early stage when they are too small to be detected using standard medical procedures. In fact, early breast cancers detected using automated screening and diagnosing systems are relatively easy to heal at this stage. Furthermore, the recent work in [69] indicate that the automated procedure is more sensitive than the manual one by a large margin, where the manual procedure achieved a 68% sensitivity ratio against a 100% ratio for the automated procedure.

D. COMPARISON WITH EXISTING LITERATURE

Surveys have been conducted in relation to application of automated systems in cancer detection such as computer aided diagnostic systems [66] with precursor attempts appearing in [68], thermography, infrared thermography and electrical impedance tomography [70], highly diversified early attempts at automated systems [71], standards and protocols to Infrared imaging technology for breast cancer detection [72], CNN based thermal imaging for breast cancer

detection [79] and various screening tools to detect breast cancer [73].

There are no emphasis on the thermal camera used, image acquisition procedures for mobile phones and public databases. This paper attempts address the gap by highlighting old and new emerging issues related to thermal imaging, the use of deep learning AI tools in aiding the diagnostic process, the use of private and public thermal image databases and the need for support for mobile phone technology. The fact that no existing solid solutions for the latter issue in the market supports our claim of lack of co mprehensive survey as presented in this paper.

E. CONTRIBUTION AND NOVELTY

The main contributions of this paper are summarized as follows. A detailed up to date narrative on breast cancer detection using thermography, that introduces new approaches using deep learning models and Artificial Neural Networks for feature extraction and classification, and highlights of thermal camera specifications used, database and image acquisition procedures. Furthermore, an introduction to research challenges, open issues and research directions for adopting AI with thermal imaging for early breast detection is presented. The novelty of this survey study is highlighting the introduction of new open issues such as: the use of mobile phone technology for patients' breast image acquisition, the use of offline cloud computing, privacy assurance, and development of new databases. This is in conjunction with detailed critique study of most of the previous studies reported in the literature covering their approach, database used, type of thermal camera, features extracted, ANN/deep learning model, results, advantages and disadvantages.

F. ARTICLE ORGANIZATION

Section II presents a brief overview of thermal camera, AI and database acquisition procedures for breast thermal images. Section III presents the details of related works on breast cancer detection using AI based on the work found in the literature. Section IV discusses open issues for research highlighting various challenges and possible research directions. Finally, the conclusion is drawn in Section V.

II. OVERVIEW

A. THERMAL CAMERA

Greeks used wet clay to apply on the area of the disease; if the particular area dries faster than other areas, it means that it has higher heat [11]. Later, the same idea evolved slowly on the use of specific measurements that indicates the existence of heat from 16th to 18 century. In 1800, Williams Herschel discovered the infrared radiation and in 1956 infrared imaging was adopted in medicine. Hence from the recent past, the thermal camera was used to diagnose the disease and detect recovery [12].

A thermal camera is a device used to detect infrared radiation from any objects having a temperature higher than absolute zero. The body which emits temperature more than absolute zero radiates electromagnetic waves. Plank equation shows the relationship between the wavelength, temperature and radiation of body surface [13]. As the range of wavelength for infrared radiation is unseen by human eyes, hence a device is required to detect this wavelength.

One of the best ways to detect the range of wavelength is by using a thermal camera. Usually, Infrared radiation contains different wavelengths between the visible range and microwave spectrum. This wavelength range of infrared radiation is between 0.75μm to 1000μm [12]. However, the wavelength range of radiation of the human body is between 8μm to 12μm (see Figure 1).

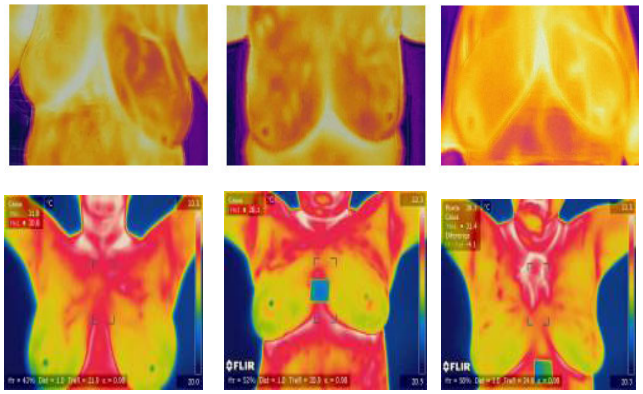

FIGURE 1. Samples of breast scan collected at a specialized hospital clinic in Sheraz Tehran for tumorous (top) and healthy (bottom) images.

The medical infrared thermography is utilized in breast abnormality detection because of its advantages such as radiation-free, non-invasive and painless nature. Infrared breast thermography is an alternative breast imaging modality that can detect early changes or tumors which cannot be detected by X-ray mammography. Breast cancer is a highly treatable disease, with 97% chances of survival if getting detected earlier [14]. Thus, early detection of breast cancer using infrared breast thermography may improve the survival rate of breast cancer patients. The temperature pattern in both breasts of a healthy breast thermogram are closely symmetrical. Hence, a small asymmetry in the temperature pattern of the left and right breast may signify a breast abnormality. There are a series of texture features that play a vital role in asymmetry analysis of breast thermograms. The use of ANN tools to classify these images as benign or malignant tumors is strongly motivated once features are selected and extracted.

B. ARTIFICIAL INTELLIGENCE

An Artificial Neural Network (ANN) is an interconnected group of smaller computational units called neurons that attempts to mimic biological Neural Networks [15]. Artificial Neural Networks and biological Neural Networks have similarities in basic things [16]. However, biological Neural Networks operate asynchronously while Artificial Neural Networks operate concurrently [17].

In 1950, AI was born when Alan Turing presented a test to determine if the computer was intelligent. AI describes the stages of development that began in 1973 when experiments failed, and research funding stopped. In the late 1980s, a series of AI experiments were conducted using the fifth-generation computer and failed to produce the expected results [18]. The 21st century has led to a paradigm shift in AI because of the vast amount of data. In 2006, Jeff Hinton published a research paper that created a spark of creativity, followed by a series of research in deep learning, which contributed to large companies such as Google, Facebook and Amazon to acquire and apply [19]. In 2010, the American Mathematical Society and the Computerized Machinery Association established AI to classify 17 types, including deep learning [18].

Deep Convolutional Neural Network specialized in image processing and consisted of two networks, the first Neural Network to extract features from images and the second Neural Network to classify the image features [20]. It is a solution to the problem of linear classification due to poor accuracy and allows the network to be more in-depth, with much fewer parameters [15]. The deep Convolutional Neural Network requires a reliable processing power resources and therefore the GPU processor is used to improve performance [21] as the color s in the picture have an impact on the performance of deep convolutional networks. In the context of deep learning, the word depth has two meanings: Depth in increasing the number of Layers in the Convolutional Neural Network and number of color s used in the analysis of the image [22] (see Figure 2).

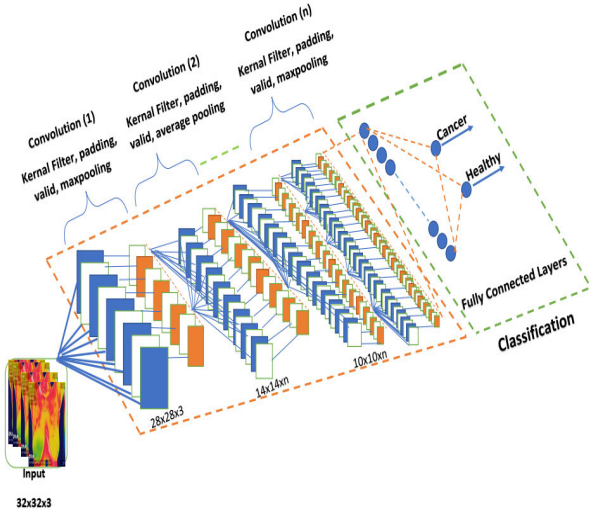

FIGURE 2. A deep convolutional neural network architecture.

C. DATABASE ACQUISITION PROCEDURE

Most of the research work on IR-thermal images use the Mastology Research with Infrared Image (DMR) database [23]. DMR-IR database has a population of 287 patients, with an age between 23 and 120 years old; 186 patients are healthy and 48 present a malignant breast. The diagnostic has been prior confirmed via mammography, ultrasound and biopsies. The thermal images are captured with a FLIR thermal camera model SC620, which has a sensitivity of less than 0.04°C and captures standard −40°C to 500°C. Each infrared image has a dimension of 640 × 480 pixels; the software creates two types of files: (i) a heat-map file; (ii) a matrix with 640 × 480 points e.g. 307200 thermal points. Firstly, each patient undergoes thermal stress for decreasing the breast surface temperature and then twenty-image sequences are captured per 5 minutes. As a thermography test may be considerably affected when guidelines are not followed, the DMR-IR database followed the Ng [24] and Satish [25] acquisition protocol, which has been gathered jointly with physicians to ensure the database's quality. Here, it is mentioned several standards that lead to high quality and unbiased thermal images. Firstly, each patient should avoid tea, coffee, large meals, alcohol and smoking before the test. Secondly, the camera needs to run at least 15 min prior to the evaluation, having a resolution of 100mK at 30°C; the camera at least should have 120 × 120 thermal points. Third, the recommended room's temperature is between 18 and 25°C, humidity between 40% and 75%, carpeted floor, avoiding any source of heat such as, personal computers, devices that generate heat and strong lights. Development of private or public breast thermal image databases require that the database is designed under strict acquisition protocols such as those discussed in [26], [23].

III. RELATED WORKS

Previous studies show that researchers used many types of thermal cameras with different specifications to detect breast cancer. Besides, it shows various types of methods to analyze and classify images, including Artificial Neural Networks. However, the different types of Artificial Neural Networks produce different accuracy levels and sensitivity ratios.

Researchers in [27] used two types of an Artificial Neural Network to detect breast cancer, which is a Backpropagation Network (BPN) and RBFN. RBFN results indicated rapid training, and high ranking compared to BPN. RBFN accuracy was 80.95%, with 100% sensitivity and 70.6% specificity in identifying breast cancer. The researchers in [28] compared the images from two thermal cameras where the first group of 27 patients photographed with thermal camera Ti40FT and the second group of 23 patients with thermal camera Varioscan 3021-ST to monitor the change in breast temperature. MRI imaging used to confirm the identification of cancer. The Ti40FT thermal camera has a sensitivity less than 0.09°C and a resolution of 160 × 120 pixels, while the Varioscan 3021-ST thermal camera has a sensitivity of 0.03 and a resolution of 360 × 200 pixels. Furthermore, the researchers [29] used different classification methods for comparison: Decision Tree (DT), Fuzzy Sugeno, Naïve Bayes Classifier, K Nearest Neighbor, Gaussian Mixture Model, and Probabilistic Neural Network. Only five features were extracted for early detection of breast cancer. The results showed that Decision Tree (DT) and Fuzzy Sugeno obtained a high accuracy of 93.30%, 86.70% sensitivity and 100% specificity.

In [30], On the other hand, the researchers used the Ti20, which is considered the same faction of thermal cameras as Ti40FT, but of lower quality as the sensitivity is only 0.2 and a resolution of 128×96 pixels. The researchers [31] extracted five Higher-order Spectral features to evaluate their use in screening for breast cancer. Two classifications used to classify normal and abnormal breast thermograms which are Artificial Neural Network (ANN) and Support Vector Machine (SVM). The results showed that SVM had a sensitivity of 76% and a specificity 84%, and the ANN seeded showed higher values of sensitivity (92%) and specificity (88%).

The researcher in [32] used the Varioscan 3021-ST model, took images of 40 patients and classified them as follows. Normal patients are 26 patient while patients with breast cancer are 14. A total of 20 extracted features from thermograms, based on Gray Level Co-occurrence Matrices, were used to evaluate the effectiveness of textural information possessed by mass regions. The ability of feature set in differentiating abnormal from normal tissue is investigated using a Support Vector Machine classifier, Naive Bayes classifier and K-Nearest Neighbor classifier. To evaluate the classification performance, five-fold cross-validation method and Receiver operating characteristic analysis was performed. The verification results show that the proposed algorithm gives the best classification results using K-Nearest Neighbor classifier and an accuracy of 92.5 %.

The researchers in [33] used the ICI7320P thermal camera on 36 patients and 22 patients, respectively. The work separated the patients into two groups. The first group contains 24 patients while the second group has 12 patients. The breast region was segmented from the thermogram images. Bispectral invariant features were obtained from Radon projections of these images. The features are then used to train a Support Vector Machine classifier to classify unseen test images into normal, benign and malignant classes. The SVM classifier classifies the normal and benign breast conditions with an accuracy of 83.3%, the normal and malignant breast conditions with the accuracy of 77.27% and benign and malignant conditions with the accuracy of 61.36%. The sensitivity is found to be 90.91% for normal and benign breast conditions, 81.82% for normal and malignant breast condition and 59.10% for benign and malignant conditions while the specificity is found to be 77.27%, 72.73% and 63.64% respectively. When the data set was expanded to contain 36 cases in each class, accuracy rates improved as follows. Normal – Benign: 91.6 %, Normal – malignant: 90.3%, Benign – Malignant: 80.6%.

In [34], Wahab *et al.* used the 7640 P high-resolution thermal camera for breast cancer patients. A series of screenings have been performed on carcinogenic induced rats and thermal images acquired were then analyzed for risk monitoring. The visual analysis has shown that the presence of hotspot and asymmetrical temperature profile could be an indicator of a high-risk patient while temperature measurement on both induced and control groups shows a significant difference in the standard deviation of the surface temperature with a smaller deviation of 0.31 ± 0.08 observed in the control group while the bigger deviation of 2.23 ± 0.78 observed in the induced group.

On the other hand, the FLIR S45 thermal camera has become widely used since 2014. In [35], the work evaluated the feasibility of using interval data in the symbolic data analysis framework to model breast abnormalities (malignant, benign and cyst) to detect breast cancer. A three-stage feature extraction approach was proposed. In the first stage, four intervals of variables are obtained by the minimum and maximum temperature values from the morphological and thermal matrices. In the second one, operators based on dissimilarities for intervals are considered and then continuous features are obtained. In the last one, these continuous features are transformed by Fisher's criterion, giving the input data to the classification process. This three-stage approach is applied to a Brazilian's thermography breast database generated using the FLIR S45 thermal camera and it is compared with statistical feature extraction and a texture feature extraction approach widely used in thermal imaging studies. Different classifiers are considered to detect breast cancer, achieving 16% of misclassification rate, 85.7% of sensitivity and 86.5% of specificity to the malignant class.

In [36], automatic detection of the regions of interest is proposed and compared with segmentations performed manually. The work presented a methodology for the automatic segmentation of lateral breast thermal images. For the evaluation of the results, different groups of ground truth are generated, which are available on the internet, to allow the verification of the results' correctness. Finally, the obtained results by the proposed methodology for the 328 FLIR S45 generated thermal images used in this work are demonstrated. The results showed average values of accuracy.

The researchers in [37] measured the breast surface temperature using the special thermal camera like FLIR SC 45. Their work focused on statistical and texture features individually giving satisfying results, these results can be improved through a combination of above features. The proposed work included advanced pre-processing stage and combined feature matrix. The pre-processing phase consists of filtering, edge detection and morphological operations. Texture and statistical features were extracted and combined feature set was used for classification. K-nearest neighbour and Support vector machine classifiers were used to classify thermal images as normal or abnormal images. DMR database which consists of breast thermal images is used to evaluate performance parameters such as sensitivity, specificity and accuracy.

The researcher [38] has built a set of networks to classify thermal images of breast cancer patients, which are Artificial Neural Networks (ANN), Decision Trees, Bayesian classifiers, Haralick and Zernike attributes, Extreme Learning Machines (ELM) and Multi-layer Perceptron (MLP). The results showed that Extreme Learning Machines (ELM) and Perceptron Multilayer (MLP) had the highest accuracies, as the sensitivity 78%, specificity 88%, and accuracy 83%.

In [39], the researchers, however, calculated the Initial Feature point Image (IFI) for each segmented breast thermogram by applying a Discrete Wavelet Transform (DWT). Then 15 types of features were extracted before being inserted into the Artificial Neural Network. Then, it is feedforward to the Multilayer Perceptron network (MLP). The achieved accuracy was 90.48%, while the sensitivity and specificity were 87.6% and 89.73%, respectively.

Thermal image analysis was carried out in [40] after converting them to grey images. A new local texture feature extraction technique, called block variance (BV), was used to extract the features in the grey images and to compare the right breast features to the left breast ones. Then feed-forward Neural Network (FANN) was used to classify them like a malignant or benign tumor. Results obtained showed an accuracy rate of 90%.

The work in [41] proposed a hybrid methodology for analyzing Dynamic Infrared Thermography to indicate patients with risk of breast cancer, using unsupervised and supervised machine learning techniques. The Dynamic Infrared Thermography quantitatively measures temperature changes on the examined surface, after thermal stress. In the Dynamic Infrared Thermography execution, a sequence of breast thermograms is generated. This sequence is processed and analyzed by several techniques. First, the region of the breasts is segmented and the thermograms of the sequence are registered. Then, temperature time series are built and the k-means algorithm is applied to these series using various values of k. Clustering formed by k-means algorithm, for each k value, is evaluated using clustering validation indices, generating values treated as features in the classification model construction step. A data mining tool was used to solve the combined algorithm selection and hyperparameter optimization (CASH) problem in classification tasks. Besides the classification algorithm recommended by the data mining tool, classifiers based on Bayesian networks, Neural Networks, decision rules and decision tree were executed on the data set used for evaluation. Test results showed among 39 tested classification algorithms, K-Star and Bayes Net presented 100% classification accuracy. Furthermore, among the Bayes Net, Multi-Layer Perceptron, Decision Table and Random Forest classification algorithms, an average accuracy of 95.38% was obtained.

The work in [56] emphasized on investigating statistical texture features to analyze breast asymmetry and signify abnormality. These features can adequately differentiate the healthy breast thermograms from pathological breast thermograms. The analysis was performed on 30 healthy and 30 abnormal breast thermograms of existing DMR (Database for Mastology Research) Database. The analysis and experimental results show that among the first-order statistical features, the mean difference, skewness, entropy and standard deviation are the most efficient features that contribute most towards the asymmetry detection.

In [42], researcher modeled the changes on temperatures in normal and abnormal breasts using a representation learning technique called learning-to-rank and texture analysis methods with multilayer perceptron (MLP) classifier. Dynamic thermal image database DMR-IR was used in the study with four experiments to evaluate the performance of the network. These experiments are the concatenation of the texture features extracted from each thermogram (without using the LTR method), the forward representation generated by the LTR method to classify the cases, the backward representation generated by the LTR method to classify the cases and the fourth experiment performed concatenate the forward and backward representations of each sequence of thermograms. Furthermore, six texture analysis methods were used, which are: Histogram of oriented gradients (HOG) method with 4 blocks and 4 cells (HOG4 $\times$ 4) HOG2 $\times$ 2 (2 blocks, 2 cells), Lacunarity analysis of vascular networks (LVN), Gabor filters (GF), Local binary pattern (LBP), Local directional number pattern (LDN) and Gray level co- occurrence matrix (GLCM). The proposed method generates a compact representation for the infrared images of each sequence, which is then exploited to differentiate between normal and cancerous cases. Results produced a competitive area under the curve (AUC = 0.989) of the receiver operating characteristic (ROC) curve. In [43], researchers analyzed infrared thermography of breast, considering distinct protocols, to classify patients images as healthy or non-healthy due to anomalies such as cancer. Belongs to DMR'' or belongs to the Database for Mastology Research (DMR)This dataset comprises static and dynamic protocols, with respect to their heat transfer. In static acquisitions, the body of the patient must achieve thermal balance in a controlled environment, while dynamic protocols are used to inspect the skin temperature recovery caused by thermal stress after cooling the patient by an electric fan. For the acquisition of thermograms, a FLIR SC-620 Thermal Camera was used. Each patient image has a spatial resolution of 640 $\times$ 480 pixels and grayscale or colored images that represents their heat temperature. Convolutional Neural Networks classifier was used obtaining 98% of accuracy for static protocol and 95% for dynamic protocol, while interestingly the accuracy in grayscale 95% and 92%, respectively.

In [14], normal and abnormal thermograms are differentiated by extracting and fusing texture features from frontal and lateral views. Multi-view thermograms are pre-processed using anisotropic diffusion. The Region of Interest from axilla to lower breast boundary is extracted through level-set segmentation without re-initialization. Texture features such as grey-level co-occurrence matrix, grey-level run-length matrix, grey-level size zone matrix and neighborhood grey tone difference matrix that quantitatively describe local or regional texture properties are extracted for 32-normal and 31-abnormal subjects chosen from DMR database. Using t-test, the reduced feature set is determined for frontal, right-lateral and left-lateral thermograms independently from the extracted texture features. Significant features are obtained by performing kernel principal component analysis on the reduced feature set. Feature fusion is performed on obtained

significant features from frontal and lateral views to obtain a composite feature vector that is fed to least square-support vector machine employing optimised hyper-parameters to classify subjects as normal and abnormal. Experimental results indicate that fusion of texture features from frontal and lateral thermograms achieved 96% accuracy, 100% sensitivity and 92% specificity.

In [44], a study of the influence of data preprocessing, data augmentation and database size versus a proposed set of CNN models were performed. Furthermore, a CNN hyperparameters fine-tuning optimization algorithm using a Tree Parzen Estimator was used. Results indicated that among the 57 patients database, the CNN models obtained a higher accuracy (92%) and F1-score (92%) that outperforms several state-of-the-art architectures such as ResNet50, SeResNet50 and Inception. The results demonstrated also that a CNN model that implements data-augmentation techniques reach identical performance metrics in comparison with a CNN that uses a database up to 50% bigger.

On the other hand, the researcher [45] selected the discriminative features for improving the classification accuracy of the infrared thermography based breast abnormality detection systems. Mann-Whitney-Wilcoxon statistical test was used to select the best discriminative features from a feature set of 24 features, extracted from each breast thermogram of DBT-TUJU and DMR databases. Three sets of features: FStat, STex and SSigFS generated from these 24 extracted features are then fed into six most widely used classifiers for comparing the efficiency of each feature set in breast abnormality detection. The experimental results show that among all three feature sets, statistically significant feature set (SSigFS) provides more accuracy in discriminating the abnormal breast thermograms from the normal.

Similarly in [46], various CNN architectures were explored for semantic segmentation starting from naive patch-based classifiers to more sophisticated ones including several variations of the encoder-decoder architecture for detecting the hotspots in the thermal image. The work showed that encoder-decoder architectures perform better when compared to patch-based classifiers in terms of accuracy, dice index, Jaccard index and inference time even with small thermal image datasets. For the first time, the thermal camera was used in the mobile phone to detect breast cancer by the researcher [47]. The model used is a FLIR with sensitivity 0.1 and resolution 80 $\times$ 60 pixels. Thermal images of 125 healthy images and 250 images of breast cancer taken. The method used extracted ROIs after background extraction, which was then compared to various features estimated from the left and right breasts using Shannon entropy and classified using logistic regression. The number of subjects in this experiment was low, to allow for precise diagnosis and to select individual features. Many misdiagnosed images occurred due to other factors, such as the subjects' menstrual period and other diseases, which result in additional heat.

Another portable S60 thermal camera with a mobile phone was used in [48] to acquire images from 78 patients, 38 images of them for patients with breast cancer. The FLIR thermal imaging camera, with the best of four (BoF) features and the support vector machine (SVM) learning classifier, was used. The 4-dimension Feature Vector (FV) is computed using the segmented image, grey Level co-occurrence matrix (GLCM) and run-length matrix (RLM) calculation. To ensure hardware optimization, the proposed multiplexed GLCM, RLM and SVM implementation realizes an area reduction of 30% compared to the conventional with minimal overhead in the system speed requirement. The Linear SVM is utilized to decide between malignant and benign based on the FV. The system is implemented on FPGA and experimentally verified using the patients from the DMR database. The breast cancer screening processor achieved the sensitivity and specificity of 79.06% and 88.57%, respectively.

Recently, few studies attempted the use of mobile phones to create breast cancer early detection systems. The researcher [49] used temperature and texture features to design a breast cancer detection system based on a smartphone with an infrared camera, achieving the accuracy of 99.21 % with the k-Nearest Neighbor classifier. The infrared images with 680 $\times$ 480 resolution were converted to grayscale images and their resolution reduced to 160 $\times$ 120, consistent with the infrared camera of the FLIR Lepton 3. The sample size classified was 1520 total patient, 760 normal patients and 760 patients with breast cancer.

A segmentation method based on a combination of the curvature function and the gradient vector flow, and for classification was used in [50], with a Convolutional Neural Network. Every breast is characterized by its shape, color, and texture, as well as left or right breast. Images of 35 normal and 28 images of cancer were analyzed. The CNN classifier results were compared to other classification techniques; tree random forest (TRF), multilayer perceptron (MLP), and Bayes network (BN). CNN presents better results than TRF, MLP, and BN, with an accuracy of 100%. Other methods (tree random forest (TRF), multilayer perceptron (MLP), and Bayes network (BN) accuracy were between 80 to 88%.

In [51], the Convolutional-Deconvolutional CNN (C-DCNN) was used to segment breast areas from 165 thermal breast images collected in house by imaging 11 breast cancer patients using the N2 Imager infrared camera. To train the C-DCNN, the inputs are 132 gray-value thermal images and the corresponding manually-cropped binary masks designating the breast areas. Cross-validation and comparison with the ground-truth images show that the C-DCNN is a promising method to segment breast areas. However, sensitivity and accuracy were not reported. The results demonstrate the capability of C-DCNN to learn the essential features of breast regions and delineate them in thermal images.

The study conducted by [52] used the new database in [48] to classify them using transfer learning with seven different deep learning pre-trained architectures: AlexNet, GoogLeNet, ResNet-50, ResNet-101, Inception V3, VGG-16 and VGG-19. Images were resized to a fixed size of 224 $\times$ 224 or 227 $\times$ 227 pixels, while the dataset was randomly split

into 70% for training and 30% for validation. The number of epochs (5) and learning rate (1×10^{-4}) were kept constant for all deep Neural Networks. VGG-16 Convolutional Neural Network outperformed with a sensitivity of 100%, specificity of 82.35% and balanced accuracy of 91.18%.

A big challenge in automated breast thermography is robust accurate segmentation of breast region against image capture errors like distance from an imaging device, view, position, etc. In [53], a cascaded CNN architecture to perform accurate segmentation robust to subject views and capture errors, is introduced. This approach can presumably detect breasts region independent of the image capture and view angle, enabling automated image and video analysis. The algorithm is compared with a multi-view heuristics-based segmentation method resulting in a dice index of 0.92 when compared with expert segmentation on a test set comprising of 900 images collected from 150 subjects at five different view angles. The classification model was hybridized by combining ResNet-50 and V-Net to analyze the thermal images. The accuracy achieved was 100% against more computational power.

The researchers in [54] introduced a comparison of deep Convolutional Neural Networks. It shows that the accuracy of inception V4 reached 80% compared to other deep Convolutional Neural Networks. Figures 1 & 2 in [55] show a comparison of 14 different deep learning models. They show that the Inception V4 achieves the highest 80% top1-crop accuracy for a small amount of operations, needed for a single forward pass, and moderate size of network parameters.

The analysis of color thermal images and the number of data used have an impact on the expected results in determining breast cancer. As CNN layers increases, the accuracy of thermal image classification increases too, but so does the complexity and run time. The classification of thermal images using CNN is a new area of research, and this has been demonstrated by fairly recent studies. Studies have shown the ability of new models to classify thermal images of breast cancer with high accuracy and high speed.

Extremely Deep Convolutional Neural Networks (DCNN) have shown their ability to improve performance further in image classification in terms of accuracy and speed too. However, there are many models in Deep Convolutional Neural Networks like Inception V1, Inception ResNet model, Inception V2, Inception V3 and Inception V4 [55]. As in the literature review, Inception V3 and InceptionResNetV2 were used to classify thermal images of breast cancer patients. Furthermore, revious studies have shown that analysis of images in grayscale format is the most common approach to feature extraction and the most common Neural Network classification model is InceptionV3. For example, in [59], the DMR database was used for a total number of patients 67, with 24 breast cancer patients and 43 healthy. The RGB color thermal images were converted to grayscale and Inception V3 deep Convolutional Neural Network was connected to a Linear Support Vector Machine to classify 1062 thermal images with 602 healthy images and the rest are having breast cancer. The Convolutional Neural Network set the learning rate at 0.0001, and the epochs to 15. The results showed that an increase in the accuracy over the number of iterations and where the training and the validation become stable after 3900 training steps. The paper emphasized that infrared imaging coupled with an agent previously administered to a patient can lead to a very accurate tumor detector. Furthermore, the classification of thermal images using deep Convolutional Neural Networks increases the quality and speed of classification.

From the dynamic thermogram DMR-IR dataset, the researcher in [57] used the total of 216 patients and divided them into 175 healthy patients and 41 sick patients with 500 healthy patients breast thermal images and another 500 sick patient thermal images. 80% of the database was used for training and 20% for validation and testing. Various models of the deep Convolutional Neural Network were used such as resnet18, resnet34, resnet50, resnet152, VGG16 and VGG19. The results indicated that resnet34 and resnet50 produced the highest validation accuracy rate of 100% for breast cancer detection.

The study conducted in [58] did initial experiments on fine-tuning the Convolutional Neural Network (CNN) models of ResNet101, DenseNet, MobileNetV2, and ShuffleNetV2 to classify healthy and sick breast cancer patients. The ImageNet database was used for testing and the dataset used to train the models are thermal breast images downloaded from the DMR database. In the training phase, three epochs were used for the training iterations 10, 20, and 30. Initially, the learning rate was set to 0.001, momentum to 0.9, learning rate factor for weight and bias each to 10, and minibatch size to 10. The results indicated that DenseNe and ResNet101 deep networks achieve an accuracy of 100% in 10 epochs only. MobileNetV2 and ShuffleNetV2, however, needed 20 epochs and 30 epochs of training, respectively, to achieve 100% accuracy. During the testing phase, however, the pre-trained model of DenseNet was able to classify all the testing dataset correctly. ResNet101 and MobileNetV2 have correctly classified static dataset while slightly missed in classifying dynamic dataset with 99.6% of accuracy. ShuffleNetV2 has a lower performance of only 98% of accuracy. ShuffleNetV2 used short training time, but MobileNetV2 with competitive elapse time demonstrated equal performance to ResNet101.

The work in [60] proposed an active contour model for the segmentation of the Suspicious regions (SRs) in thermal breast images (TBIs). The proposed segmentation method comprises three steps. First, a novel method, called smaller-peaks corresponding to the high-intensity-pixels and the centroid-knowledge of SRs (SCH-CS), is proposed to approximately locate the SRs, whose contours are later used as the initial evolving curves of the level set method (LSM). Second, a new energy functional, called different local priorities embedded (DLPE), is proposed regarding the level set function. DLPE is then minimized using the interleaved level set evolution to segment the potential SRs in a TBI more

accurately. Finally, a new stopping criterion is incorporated into the proposed LSM. The proposed LSM increases the segmentation speed and ameliorates the segmentation accuracy. Feed-forward Artificial Neural Network with 42 neurons and 0.1 learning rate was used for the classification of thermal images. Performance of the SR segmentation method was evaluated on two DMR-IR and DBT-TU-JU databases and the average segmentation accuracies obtained on these databases are 72.18% and 71.26%, respectively. Experiments show that investigating only the SRs instead of the whole breast is more effective in differentiating abnormal and normal breasts.''

Researchers in [61] took an interesting approach to estimate the position and size of a spherical tumour in a human breast using the temperatures obtained on the surface of the breast through a breast thermogram in conjunction with Artificial Neural Networks. The surface temperature was obtained using numerical simulation of heat conduction in a cancerous breast by employing the Pennes bio-heat transfer equation using a finite element based commercial solver COMSOL. The surface temperatures are then trained against the tumour parameters by using Artificial Neural Networks (ANN). The Artificial Neural Network is composed of two hidden layers. In addition, out of 447 thermal data vectors, 375 vectors were used for training and 72 vectors for testing. Random noise was added at different rates so that the thermal images depend on the accuracy of the infrared camera used. The results indicated that for the'measured' data without noise, accuracies of 90% in position and 95% in the radius for the constant heat generation rate were estimated using ANN. Adding the noise, however, drops the accuracies to 88% and 98%, respectively. Similar recent attempts on resolving the depth of emissive tissue in breast using numerical modelling was reported in [74]–[76].

Researcher in [64] highlighted the effect of menstruation period on the stability of temperature, which affects the result of the prediction. Two experiments were performed on 200 patients, they were divided into two groups, where the first group included all patients, and the second group was thermal imaging in the recommended day of menstruation, e.g., day 5, 12 and 21 of menstruation. The results indicated that the second group was more accurate than the first one because body temperature was predictably more stable in the second group. The second experiment was made using the Artificial Neural Network. The mean, median and modal temperatures of healthy breasts, and mean, median, mode, SD and skewness of an unhealthy individual were highly correlated. Hence, these values are used as the ANN training sets. Four Artificial Neural Networks were used according to above inputs, setting Momentum of 0.4 and Learning rate of 0.5. The learning index was the root mean-squared (rms) error, which determined if the network was properly tested. The results showed that the Artificial Neural Network (inputted with information on mean, median and modal temperatures of both breasts, age, family history, hormone replacement therapy, age of menarche, presence of palpable lump, previous surgery/biopsy, presence of nipple discharge, breast pain, menopause at age <50 years, and first child at age <30 years of the patient) converges best during training and gives the highest accuracy when tested.

In [65], researchers used the thermography database from a Singapore Hospital, which used thermal camera model NEC-Avio Thermo TVS2000 MkIIST with 0.1 sensitivity. Accordingly, 90 patients were chosen randomly to undergo the thermography examination where the room temperature ranged from 20 to 22. In addition, a patient wearing a loose robe were made to rest for 15 minutes before the experiment. The analysis was also conducted for 25 breast cancer patients and 25 healthy persons. The data was divided into three parts; two parts for training and one part for testing. In addition, features of moment1, moment3, run percentage, and gray level non-uniformity were selected, as they were clinically significant (low p-values) compared to the other features, and inserted into the SVM for classification. A diagnostic test was assessed by determining the AAUC, which can vary between 0.5 and 1. The results indicated that the use of only four features gives a high accuracy of 88.10%, sensitivity of 85.71% and specificity of 90.48%.

However, in [67], only 50 thermal images were used, out of which 25 are cancer-related thermograms, and 25 are healthy-related thermograms. The reduced image size of the 64 * 64-pixel size was used with Decision Tree, Discriminant, k-Nearest Neighbour and Fuzzy Sugeno, Naive Bayes, SVM, AdaBoost, and Probabilistic Neural Network classifiers. The results indicated that the Decision Tree classifier is able to identify the breast cancer with an average accuracy, sensitivity, specificity and area under curve of 98%, 96.66%,100% and 0.98 respectively. In addition, results show that the system requires only two features for correct identification of normal and malignant breast thermograms. Notably, the paper claims the first to attempt using HOG descriptors for the detection of breast cancer while obtaining the highest classification performance compared to other existing methods.

In [78] researcher used DCNN to detect breast cancer. The analysis was performed on 521 healthy and 160 abnormal breast thermograms of existing DMR Database. Obtained color thermal images were converted to grayscale, pre-processed, segmented, and classified using DCNN. Moreover, SGD optimization method and learning rate 0.01 were used. Results indicate an increase in the accuracy ratio from 93.3% to 95.8%, while sensitivity and specificity levels were at 99.5% and 76.3%, respectively.

IV. OPEN ISSUES

Table 1 shows a comprehensive comparison between different studies of early breast detection methods together with camera type, sample size, and results. In the literature review, the researchers pointed out the use of high-tech computers to store and process thermal images. However, this technology has challenging problems, including damaged data, while the data is subject to lose or theft in the case of transfer, in addition to costly storage devices. It is clear that mobile phones are portable computers, so they are developed to

TABLE 1. Comparison between different methods of early breast detection.

Study	Camera type	Patients		AI used	Features	Type of image	Acc%	Spe %	Sens %	AUC%
		N	S							
[27]	TVS-2000	30	52	RBFN	mean, median, standard deviation	Color	80.95	70.6	100	98.8
[29]	TVS2000	25	25	KNN	One clinically significant texture (Energy, Contrast, Homogeneity, Entropy and Angular second moment) and two DWT features (Average Dv1 and Energy)	Grayscale	90	93.3	86.7	NG
				PNN			90	93.3	86.7	NG
[31]	TVS2000	25	25	ANN+SVM	Mean of Magnitude and three Phases Entropy for higher-order spectra (HOS).	Grayscale	90	88	92	NG
[32]	VARIOSCAN 3021 ST	26	14	KNN	20 Textural features (Energy, Contrast, Correlation, Variance, Homogeneity, Sum Average, Sum Variance, Sum Entropy, Entropy, Difference Variance, Difference Entropy, Information Measure of Correlation 1, Information Measure of Correlation 2, Autocorrelation, Dissimilarity, Cluster Shade, Cluster Prominence, Maximum Probability, Inverse Difference Normalized, Inverse Difference Moment Normalized)	Grayscale	92.5	NG	NG	NG
[33]	ICI7320P	24	12	SVM	First-order statistical features (mean, variance, skewness and kurtosis) and texture features (ASM, Contrast, Correlation, Sum of squares, Inverse difference moment, Sum average, Sum variance, Sum entropy, Entropy, Difference variance, Difference entropy, Information Measure of Correlation 1, Information Measure of Correlation 2)	Grayscale	83.3	NG	NG	NG
[34]	7640 P-Series	NG	NG	NOT USED	Symmetrical profile, Obvious hotspot and Overall changes	Color	NG	NG	NG	NG
[36]	FLIR S45	Total = 180		NOT USED	NG	Grayscale	NG	NG	NG	NG
[35]	FLIR S45	Total = 50		NOT USED	proposed three- stage feature extraction (PFE), statistical feature extraction (SFE) and texture feature extraction (TFE)	Grayscale	NG	86.5	85.7	NG
[38]	FLIR S45	227	235	Extreme Learning Machines	Texture features and geometry of lesions features	Grayscale	83	88	78	NG
[39]	FLIR SC-620	183	123	Artificial Neural Network	Mean values of the feature point and Statistical feature extraction	Grayscale	90.48	89.73	87.6	NG
[40]	FLIR SC-620	60	40	feed-forward Artificial Neural Network (FANN)	16 texture features	Color	90	85	95	95.3
[56]	FLIR SC-620	30	30	NOT USED	first order statistical features (the mean difference, skewness, entropy and standard deviation)	Grayscale	97	NG	NG	NG
[42]	FLIR SC-620	19	37	LTR+MLP Multi-layer Perceptron	Texture Feature (Autocorrelation, Contrast, Correlation I, Correlation II, Cluster prominence, Cluster shade, Dissimilarity, Energy, Entropy, Homogeneity I, Homogeneity II, Maximum probability, Sum of squares, Sum average, Sum entropy, Sum variance, Difference variance, Difference entropy, Information measure (IM) of correlation I, IM of correlation II, Inverse difference (ID) normalized and ID moment normalized.	Grayscale	95.8	NG	97.1	98.9
[44]	FLIR SC-620	19	37	ResNet50, SeResNet50 Inception	texture and statistical features	Grayscale	92	94	91	92
[46]	FLIR SC-650	Total = 1200		V net	high-level features	Grayscale	99.6	NG	99.6	NG
[49]	FLIR Lepton 3	760	760	KNN	four texture features (the contrast, inverse different moment, entropy, energy)	Grayscale	99.21	100	98.4	NG
[50]	FLIR SC-620	35	28	CNN with (TRF, MLP, and BN)	Texture Features (Shape: Area, Perimeter, Roundness and Compactness. First-order texture: Average, Median, Variance, Standard deviation and Entropy. Second-order texture: Contrast descriptor, Correlation, Energy and Local homogeneity. Relation context: Euclidian distance, Bhattacharyya distance and Difference.)	Color	100	100	NG	100
[14]	FLIR SC-620	32	31	LSSVM +RBF	Texture features such as grey-level co-occurrence matrix, grey-level run-length matrix, grey-level size zone matrix and neighbourhood grey tone difference matrix	Grayscale	96	92	100	96
[37]	FLIR SC 45 + FLIR SC-620	NG	NG	KNN +SVM	texture features (Contrast, Energy, Homogeneity and Correlation). statistical features (Mean, Standard deviation, Skewness and Kurtosis).	Grayscale	NG	NG	NG	NG
[41]	FLIR SC-620	40	40	Bayes Net	Feature selection methods: Best First, Greedy Stepwise, Ranker, Correlation-based Feature Selection (CFS) Subset Eval, Pearson Correlation Eval, Gain Ratio Eval, Info Gain Eval, 1-R Eval, Principal Components Eval, RELIEF Eval, Symmetrical Uncertainty Eval.	Grayscale	100	100	NG	100
				Bayes Net, multi-layer perceptron, decision table and random forest classification algorithms			95.38	95.37	NG	95
[43]	FLIR SC-620	95	42	CNN	automatic feature selection	Grayscale	95 by dynamic	NG	NG	NG
		95	42	CNN		Color	98 by static	NG	NG	NG

TABLE 1. *(Continued.)* **Comparison between different methods of early breast detection.**

[47]	FLIR One	125	125	ANN	Twelve color features were used for classification including mean, variance, skewness, and kurtosis	Grayscale Color	NG	50	98.6	NG
	FLIR A320	125	125	ANN	Twenty features, including energy, entropy, contrast, homogeneity and correlation of horizontal, vertical, diagonal, and anti-diagonal directions		NG	50	98.6	NG
[48]	CAT S60	Total = 7800		LSVM and CNN	Best of five (BoF) features selected from texture features	Grayscale	90.5	91.8	90.06	NG
[51]	N2 Imager	0	11	C-DCNN	automatic feature extraction	Grayscale	NG	NG	NG	NG
[52]	FLIR SC-620	141	32	VGG-16	NG	NG	91.18	82.35	100	84.52
[45]	FLIR T650sc	24	46	SVM_RBF	Three set of features: FStat, STex and SSigFS	Color	84.29	87.50	82.60	NG
	FLIR SC-620	45	35				85.00	80.00	90.00	NG
	FLIR T650sc	24	46	ANN			84.29	75.00	89.13	NG
	FLIR SC-620	45	35				87.50	93.33	80.00	NG
[53]	NG	Total = 1260		Hybrid (ResNet-50 and V-Net)	high-level features	Grayscale	100	NG	NG	NG
[58]	FLIR SC-620	static		ResNet101 DenseNet	NG	NG	100	NG	NG	NG
		2595		698						
		dynamic				NG	100	NG	NG	NG
		255		33						
[57]	FLIR SC-620	500		500	resnet34	Color	100	NG	NG	NG
					resnet50	Color	100	NG	NG	NG
[59]	FLIR SC-620	43		24	Inceptionv 3 + LSVM	NG	Grayscale	NG	NG	NG	NG
[60]	DMR-IR and DBT-TU-JU	35		30	FANN	Haralick features and Hu's moment invariants	Grayscale	88.5	89	87	93.9
		46		44						
[61]	NG	NG		NG	ANN	NG	Color	95%	NG	NG	NG
[62]	Thermov ision 680 Medical	Total =19			ANN	mean, standard deviation, median, maximum, minimum, skewness, kurtosis, entropy, area and heat content	Grayscale	NG	NG	NG	NG
[63]	FLIR SC-620	48		46	ANN	mean, variance, standard deviation (SD), skewness, kurtosis, entropy, range and median	Grayscale	85	83	87	NG
[64]	NG	76		131	ANN	mean, median, modal, SD and skewness temperature of both breasts	NG	NG	NG	NG	NG
[65]	Thermo TVS200 0 MkIIST	25		25	SVM	moment1, moment3, run percentage, and gray level non-uniformity	Grayscale	88.10	90.48	85.71	88.1
[67]	Thermo TVS200 0 MkIIST	25		25	Decision Tree	HOG	Grayscale	98	100	96.66	98
[78]	FLIR SC-620	521		160	DCNN	NG	Grayscale	95.8	76.3	99.5	NG

keep pace with virtual reality, and the developments taken place in mobile cloud computing. Mobile Cloud Computing is a hybrid of cloud computing and mobile devices that is considered to have the ability to overcome these limitations.

Mobile cloud computing provides many advantages, including a high processing capability and a huge storage capacity equipped with configurable computing resources for users to perform calculations. It can also update data instantly on the cloud and on the mobile phone by synchronization and provide security to protect data confidentiality and integrity. Besides, it is inexpensive compared to high-specs computers. Through mobile cloud computing, thermal images are processed, and the results are sent to the mobile application.

One of the most challenges is the quality of the thermal image, so the most critical step in processing thermal images is enhancing the image. Enhancements are processes used to show hidden details and highlight the features in the thermal image so that the depth and size of the tumor may be distinguished from a healthy tissue. If the tumor is close to the surface, it is easier to discover. However, one needs to enhance the contrast of the thermal image to distinguish the tumor from healthy tissue, if the tumor location is deep. One of the proposed methods is to use a breast cooling device such as Ice Pack Gel for a specific period to improve the image quality and detect the tumor using a lower resolution thermal camera unlike expensive thermal cameras.

The above issue is further exacerbated with the use of mobile phones with mounted thermal cameras. Having no standardized thermal image acquisition procedures for the mobile phone, results in low quality, offset, jerky images

produced that are hard to process and may result in nullifying them. Therefore, on top of standardized image acquisition procedures required (to regulate issues like stability of thermal camera, distance from the patient's breast, room temperature and humidity, light intensity, acquisition angle, patient's pose, prior resting of patient's body, alcohol and hot beverage consumption, application of topical creams, hair shaving, etc.), further sophisticated image enhancement techniques are needed. Without such regulations and strictly followed acquisition procedure rules, in conjunction with image enhancement techniques, the dream of having early breast cancer detection from the comfort of the patient's room may not become a reality soon.

Computer-based methods for clinically diagnosing thermal images of breast cancer patients lead to many complications in breast cancer care system. Some studies show inability to accommodate the increasing numbers of patients with breast cancer, which causes a significant burden on the radiologist, delaying diagnosis and causing long waiting for patients. Additionally, it causes a decrease in the quality of medical care with patient distress and anxiety. Moreover, sometimes doctors make mistakes, and computer fails to keep up with the update of the databases. Therefore, computation complexity needs to be pushed to the cloud to support smartphone applications development, which facilitates the process of self-diagnosis at home.

It is evident from previous studies that researchers made a great effort in using different models of ANN and recently deep learning for early detection of breast cancer. Table 1 and 2 present the details of the reported studies from the open literature such as: type of thermal cameras used, database, acquisition procedure (if any), sample size (e.g., number of patients, healthy individuals, and breast images used), deep learning model, types of extracted features, type of images used, performance evaluation metrics, and advantages and disadvantages. However, previous studies were limited to varying the numbers of thermal images used mostly from DMR-IR database. In addition, it included various types of thermal cameras used on several breast-cancer patients and healthy individuals. Several different types of Artificial Neural Networks (ANNs) and deep learning models were compared in table 1 to process thermographic images of breast cancer, such as RBFN, K-Nearest Neighbors (KNN), Probability Neural Network (PNN), Support Vector Machine (SVM), ResNet50, SeResNet50, V Net, Bayes Net, Convolutional Neural Networks (CNN), Convolutional and DeConvolutional Neural Networks (C-DCNN), VGG-16, Hybrid (ResNet-50 and V-Net), ResNet101, DenseNet and InceptionV3. ANNs extract different number of sets of features while deep learning models utilize automatic feature extraction for thermal image classification. A parameter evaluation is usually used to verify the performance of these Neural Networks. The analysis of the literature indicate that several factors do affect the performance of the Neural Network used, such as Database, optimization method, Neural Network model and the extracted features. However, most of the ANNs and deep learning models studied achieve a classification accuracy of 80% to 100%.

Through this evaluation in Table 1, it is clear that the percentage of accuracy in detecting breast cancer depends on several factors, such as preprocessing of thermal images used in training and testing, type of deep learning model used, number and type features extracted, the nature of image used (e.g., colored or greyscaled), while the most crucial factor for determining the accuracy is the sample size. In most of the reported previous studies, the sample size is small leading to over-claimed accuracy levels reported (e.g., a 100%). Furthermore, the objective should not be a 100% accurate detection system for the early breast cancer. Rather, the system should be designed as an assistant for the diagnosing physician to mitigate or flag a human error (e.g., final diagnostic decision should be made by the doctor rather than the system). In addition, it is necessary to find performance evaluation values to verify the efficiency of models used such as: sensitivity, AUC, and specificity. These metrics were not always reported in the previous studies. Moreover, some of the deep learning models used, such as V net and VGG16, were time consuming and require larger memory size and computational power to process, compared to, for example, Inception V3.

As we have noted previously, thermal cameras can monitor thermal changes in blood vessels. Therefore, the future work in the detection of breast cancer is related to four major issues: lower resolution thermal cameras suitable for mobile phone, error-tolerant robust image acquisition procedures for accurate breast region segmentation, classification Neural Network used (e.g., CNN vs deep CNN), and more comprehensive database.

There are three main factors in choosing a thermal camera: sensitivity, quality and price. All factors influence the choice of the thermal camera by researchers, so the thermal camera model SC620 is the most used during the past ten years. Its advantages are as follows: Sensitivity is less than 0.04, the quality is 640×480, and the price is high. Many models of thermal cameras characterized by high sensitivity and resolution can be used to detect breast cancer in an early stage. Examples of such thermal camera model is the FLIRX8500sc, that is characterized by the resolution of 1280×1024 and the sensitivity ratio 0.02°C, and it can be used in future work. The acquired images are 14-bit which contain a lot of information.

On the other hand, there are many models of a small thermal camera that can be connected to mobile phones or computer directly with excellent sensitivity and resolution. Thermal cameras are still newly produced and have a promising future. From the above studies, the ability to detect breast cancer using thermal cameras accurately is higher with better sensitivity and higher quality images. However, the camera cost remains prohibitive. Furthermore, some of these camera models are obsolete now.

In Neural Networks, future work is needed to detect breast cancer by using Recurrent Neural Network method. Recurrent Neural Network method has many models, such as

TABLE 2. Advantages and disadvantages different methods of early breast detection.

Study	Advantages	Disadvantages	Study	Advantages	Disadvantages
[27]	RBF networks are fast, robust and more tolereant than traditional Neural Networks. Sensitivity ratio and AUC are high. Color thermal images used.	Other Neural Networks can achieve better classification results networks. Sample size is small. Few features are used.	[41]	High resolution thermal camera used. Large number of features used. Accuracy ratio and AUC are high.	Sensitivity not given. Sample size is small.
[29]	KNN has simple implementation. Robust with regard to the search space.	Sample size is small. Few features used. The sensitivity is low. Model is sensitive to noisy or irrelevant attributes, which can result in less meaningful distance numbers.	[43]	High resolution thermal camera used. High classification accuracy. Automated extraction feature used.	Sensitivity not given. Sample size is small.
	PNN is robust with regard to the search space.	Requires large memory space. Thermal camera has low resolution. Sample size is small. Few features used. Sensitivity is low.	[47]	Large number of features used. Sensitivity ratio is high.	Thermal camera has low resolution. Sample size is small. Accurecy not given.
[31]	Model has high accuracy.	Sample size is small. Few features used. Sensitivity is low.	[48]	Sample size is large. Accuracy ratio and Sensitivity are high.	Thermal camera has low resolution. AUC not given. Few features are used.
[32]	Simple implementation. Robust with regard to the search space. Large number of features used.	Thermal camera has low resolution. Sample size is small. Few features used. Sensitivity not given. Model is sensitive to noisy or irrelevant attributes, which can result in less meaningful distance numbers. Model is non parametric.	[51]	Automated extraction feature used.	Sensitivity, sample size, accuracy, AUC are not given. Sample size is small Thermal camera has low resolution.
[33]	Large number of features used. Classification accuracy is high. Low generalization error.	Thermal camera has low resolution. Sample size is small. Few features used. Sensitivity not given. Accuracy is low.	[52]	High resolution thermal camera used. High classification accuracy. Sensitivity ratio is high.	Sample size is small. Features not given.
[34]	Not relevant.	Thermal camera has low resolution. Sample size is small. Sensitivity not given. Accurecy not given. No AI model used.	[45]	High resolution thermal camera used. RBF networks are fast, robust and more tolereant than traditional Neural Networks. High accuracy. Color thermal images used.	Thermal camera has low resolution. Sample size is small. Few features are used.
[36]	Not relevant.	Thermal camera has low resolution. Sample size is small. Sensitivity not given. Accurecy not given. No AI model used.	[53]	Sample size is large. Automated extraction feature used.	Sensitivity not given. Model is time consuming. Thermal camera not given.
[35]	Not relevant.	Thermal camera has low resolution. Sample size is small. Sensitivity not given. Accurecy not given. No AI model used.	[58]	High resolution thermal camera used. Sample size is large. High accuracy.	Sensitivity not given. Model is time consuming. Features are not given.
[38]	Short trining time.	Thermal camera has low resolution. Sample size is small. Sensitivity is low. Accuracy is low	[57]	High resolution thermal camera used. Sample size is large. High accuracy. Color thermal images used.	Sensitivity not given. Model is time consuming. Features are not given.
[39]	High resolution thermal camera used. High classification accuracy.	Sample size is small. Sensitivity is low. Model is time consuming.	[59]	High resolution thermal camera used.	Sample size is small. Sensitivity, accuracy, AUC are not given.
[40]	High resolution thermal camera used. High accuracy. Large number of features used.	Sample size is small. Sensitivity is low. Model is time consuming.	[60]	High resolution thermal camera used. Accuracy ratio and Sensitivity are high.	Sample size is small. Few features are used.
[56]	High resolution thermal camera used. High accuracy.	No AI model used. Sample size is small. Sensitivity not given.	[61]	Color thermal images used. Classification accuracy is high.	Sensitivity not given. Features are not given. Thermal camera not given. Features are not given.
[42]	High resolution thermal camera used. Large number of features used.	Sample size is small. Model is time consuming.	[65]	Accuracy ratio and AUC are high.	Sample size is small. Few features are used.
[44]	High resolution thermal camera used. Sensitivity ratio and Accuracy are high.	Sample size is small. Model is time consuming and high cost compution.	[67]	Accuracy ratio and AUC are high.	Sample size is small. Few features are used.
[46]	High resolution thermal camera used. Sensitivity ratio and Accuracy are high.	Model is time consuming with high computational cost.	[64]	Not relevant	Sensitivity not given. Sample size is small. Accurecy not given. Thermal camera not given.
[49]	KNN has simple implementation. Robust with regard to the search space.	Thermal camera has low resolution. Sample size is small. Few features used. Model is sensitive to noisy or irrelevant attributes, which can result in less meaningful distance numbers.	[63]	High resolution thermal camera used.	Sample size is small. Few features are used.
[50]	High resolution thermal camera used. Classification accuracy is high. Large number of features used.	Sensitivity not given. Thermal camera has low resolution. Sample size is small. Model is sensitive to noisy or irrelevant attributes, which can result in less meaningful distance numbers	[62]	Large number of features used.	Thermal camera has low resolution. Sensitivity not given. Sample size is small. Accurecy not given. Few features are used.

TABLE 2. ***(Continued.)*** **Advantages and disadvantages different methods of early breast detection.**

[14]	High resolution thermal camera used. RBF networks are fast, robust and more tolereant than traditional Neural Networks. Sensitivity ratio and AUC are high. Color thermal images used.	Sample size is small. Few features are used. Thermal camera has low resolution.	[53]	Sample size is Large . Automated extraction feature used.	Sensitivity not given. Model is time consuming. Thermal camera not given.
[37]	High resolution thermal camera used. Robust with regard to the search space.	Sensitivity, sample size, accuracy, AUC are not given.	[78]	High resolution thermal camera used. Sensitivity ratio and Accuracy are high.	Sample size is small. AUC is not given. Features are not given. Model is time consuming.

Gated Recurrent Unit (GRU, Bi-directional RNN (B-RNN) and Neural Turing Machines (NTM), which are used to detect breast cancer in an early stage.

On the other hand, works on Deep Convolutional Neural Networks is intensifying. Future works should concentrate on the use of high sophisticated Deep Convolutional Neural Networks; such as inception Resnet models. This newly established network resembles a vast area for research and quality verification in the early detection of breast cancer.

In conclusion, the data are still outdated and have not been updated. Besides, the images are captured with thermal cameras of lower quality than those currently available ones. Breast Thermal images in the database are available from limited countries only. Therefore, future work needs to find the data of thermal images of the breasts using thermal cameras, which are characterized by superior quality and sensitivity. Also, thermal images are taken from a range of states so that they include data for different breast sizes and shapes. With the advancements in deep learning models and the mobile technology, authors believe that rising sophisticated AI tools will serve as an excellent physician assistant in making accurate and early diagnostic decisions, saving lives, rather than replacing him.

V. CONCLUSION

This paper has provided a systematic review of research works dealing with AI models in conjunction with thermography for early breast cancer detection. Four major issues were highlighted from the study, namely: the small sample size used in the experiments, the heavy dependence on the DMR-IR database, image enhancement techniques applied and the limited number of advanced deep learning models. The review study highlighted the validity and potential of using theromography for early breast cancer detection by capturing the differences in thermal distribution across the breast tissue. Image enhancement techniques could be used to further locate the ROI in a 3D volume. Furthermore, the study indicated that ANN and deep learning models could achieve an acceptable level of detection accuracy but they can be improved.

Open issues highlighted the need for mobile cloud computing and elaborated on the challenges faced for such a paradigm shift in diagnosis from a computer-based tool to a smartApp. It is interesting to highlight that the research area is open for tremendous development efforts with the great advances made by deep learning models and might hold the key to huge commercial potential. However, standards and procedures for image acquisition from portable devices, camera specs, and awareness that fact that these tools are to aid physicians rather than to replace them, is of paramount importance.

REFERENCES

[1] R. Lakhtakia, "A brief history of breast cancer: Part I: Surgical domination reinvented," *Sultan Qaboos Univ. Med. J.*, vol. 14, no. 2, pp. 166–169, 2014.

[2] B. W. C. Amalu, "A review of breast thermography," *Int. Acad. Clin. Thermol.*, p. 112, 2003. [Online]. Available: https://www.iact-org.org/articles/articles-review-btherm.html

[3] R. Lakhtakia, "A brief history of breast cancer: Part I: Surgical domination reinvented," *Sultan Qaboos Univ. Med. J.*, vol. 14, no. 2, pp. 166–169, 2014.

[4] H. Koch, "Mammography as a method for diagnosing breast cancer," *Radiologia Brasileira*, vol. 49, no. 6, p. 7, Dec. 2016, doi: 10.1590/0100-3984.2016.49.6e2.

[5] P. J. Dempsey, "The history of breast ultrasound," *J. Ultrasound Med.*, vol. 23, no. 7, pp. 887–894, Jul. 2004, doi: 10.7863/jum.2004.23.7.887.

[6] D. A. Kennedy, T. Lee, and D. Seely, "A comparative review of thermography as a breast cancer screening technique," *Integrative Cancer Therapies*, vol. 8, no. 1, pp. 9–16, Mar. 2009, doi: 10.1177/1534735408326171.

[7] X. Yao, W. Wei, J. Li, L. Wang, Z. Xu, Y. Wan, K. Li, and S. Sun, "A comparison of mammography, ultrasonography, and far-infrared thermography with pathological results in screening and early diagnosis of breast cancer," *Asian Biomed.*, vol. 8, no. 1, pp. 11–19, Feb. 2014, doi: 10.5372/1905-7415.0801.257.

[8] A. Hossam, H. M. Harb, and M. A. E. K. Hala, "Performance analysis of breast cancer imaging techniques," *Int. J. Comput. Sci. Inf. Secur.*, vol. 15, no. 5, pp. 48–56, 2018.

[9] S. P. Power, F. Moloney, M. Twomey, K. James, O. J. O'Connor, and M. M. Maher, "Computed tomography and patient risk: Facts, perceptions and uncertainties," *World J. Radiol.*, vol. 8, no. 12, p. 902, 2016, doi: 10.4329/wjr.v8.i12.902.

[10] A. Bhide, S. Datar, and K. Stebbins, "Case histories of significant medical advances: Gastrointestinal endoscopy," Harvard Bus. School Accounting Manage. Unit Working Paper 20-005, Jul. 2020. [Online]. Available: https://ssrn.com/abstract=3429986 or http://dx.doi.org/10.2139/ssrn.3429986

[11] T. L. Williams, *Thermal Imaging Cameras Characteristics and Performance*, vol. 53, no. 9. London, U.K.: CRC Press, 2013.

[12] H. Qi and N. A. Diakides, *Thermal Infrared Imaging in Early Breast Cancer Detection*. London, U.K.: Springer, 2009.

[13] R. Gade and T. B. Moeslund, "Thermal cameras and applications: A survey," *Mach. Vis. Appl.*, vol. 25, no. 1, pp. 245–262, Jan. 2014, doi: 10.1007/s00138-013-0570-5.

[14] V. Madhavi and C. B. Thomas, "Multi-view breast thermogram analysis by fusing texture features," *Quant. Infr. Thermography J.*, vol. 16, no. 1, pp. 111–128, Jan. 2019, doi: 10.1080/17686733.2018.1544687.

[15] H. H. Aghdam and E. J. Heravi, *Guide to Convolutional Neural Networks: A Practical Application to Traffic Sign Detection and Classification*. Cham, Switzerland: Springer, 2017.

[16] J. Heaton, *Articial Intelligence for Humans: Deep Learning and Neural Networks and Deep Learning*, vol. 3. USA: Heaton Research, 2015.

[17] S. Khan, H. Rahmani, S. A. A. Shah, and M. Bennamoun, "A guide to convolutional neural networks for computer vision," *Synth. Lectures Comput. Vis.*, vol. 8, no. 1, pp. 1–207, Feb. 2018.

[18] S. Skansi, "Introduction to learning," in *From Logical Calculus to Artificial Intelligence*. Cham, Switzerland: Springer, 2018, doi: 10.1007/978-3-319-73004-2.

[19] J. Patterson and A. Gibson, *Deep learning: A Practionar Approach*. Newton, MA, USA: O'Reilly Media, 2017.

[20] P. Kim, *MATLAB Deep Learning: With Machine Learning, Neural Networks and Artificial Intelligence*. South Korea: Apress, 2017, doi: 10.1007/978-1-4842-2845-6.
[21] C. C. Aggarwal, *Neural Networks and Deep Learning*. Cham, Switzerland: Springer, 2018, doi: 10.1007/978-3-319-94463-0.
[22] A. Glassner, *Deep Learning: From Basics to Practice*, vol. 2. Seattle, WA, USA: The Imaginary Institute, 2018.
[23] L. F. Silva, D. C. M. Saade, G. O. Sequeiros, A. C. Silva, A. C. Paiva, R. S. Bravo, and A. Conci, "A new database for breast research with infrared image," *J. Med. Imag. Health Informat.*, vol. 4, no. 1, pp. 92–100, Mar. 2014, doi: 10.1166/jmihi.2014.1226.
[24] E. Y.-K. Ng, "A review of thermography as promising non-invasive detection modality for breast tumor," *Int. J. Thermal Sci.*, vol. 48, no. 5, pp. 849–859, May 2009, doi: 10.1016/j.ijthermalsci.2008.06.015.
[25] S. G. Kandlikar *et al.*, "Infrared imaging technology for breast cancer detection—Current status, protocols and new directions," in *International Journal of Heat and Mass Transfer*, vol. 108. Amsterdam, The Netherlands: Elsevier, 2017, pp. 2303–2320, doi: 10.1016/j.ijheatmasstransfer.2017.01.086.
[26] M. K. Bhowmik, U. R. Gogoi, K. Das, A. K. Ghosh, D. Bhattacharjee, and G. Majumdar, "Standardization of infrared breast thermogram acquisition protocols and abnormality analysis of breast thermograms," in *Proc. Thermosense, Thermal Infr. Appl.*, vol. 9861, May 2016, Art. no. 986115, doi: 10.1117/12.2223421.
[27] E. Y. K. Ng and E. C. Kee, "Advanced integrated technique in breast cancer thermography," *J. Med. Eng. Technol.*, vol. 32, no. 2, pp. 103–114, Jan. 2008, doi: 10.1080/03091900600562040.
[28] V. Umadevi, S. V. Raghavan, and S. Jaipurkar, "Interpreter for breast thermogram characterization," in *Proc. IEEE EMBS Conf. Biomed. Eng. Sci. (IECBES)*, vol. 1, Nov. 2010, pp. 150–154, doi: 10.1109/IECBES.2010.5742218.
[29] M. R. K. Mookiah, U. R. Acharya, and E. Y. K. Ng, "Data mining technique for breast cancer detection in thermograms using hybrid feature extraction strategy," *Quant. Infr. Thermography J.*, vol. 9, no. 2, pp. 151–165, Dec. 2012, doi: 10.1080/17686733.2012.738788.
[30] D. Nurhayati, T. S. Widodo, and A. Susanto, "Detection of the breast cancer from thermal infrared images," *J. Sist. Komput.*, vol. 1, no. 2, pp. 65–70, 2011.
[31] U. R. Acharya, E. Y. K. Ng, S. V. Sree, C. K. Chua, and S. Chattopadhyay, "Higher order spectra analysis of breast thermograms for the automated identification of breast cancer," *Expert Syst.*, vol. 31, no. 1, pp. 37–47, Feb. 2014, doi: 10.1111/j.1468-0394.2012.00654.x.
[32] M. Milosevic, D. Jankovic, and A. Peulic, "Thermography based breast cancer detection using texture features and minimum variance quantization," *EXCLI J.*, vol. 13, pp. 1204–1215, Nov. 2014, doi: 10.17877/DE290R-7338.
[33] S. V. Francis, M. Sasikala, G. B. Bharathi, and S. D. Jaipurkar, "Breast cancer detection in rotational thermography images using texture features," *Infr. Phys. Technol.*, vol. 67, pp. 490–496, Nov. 2014.
[34] A. A. Wahab, M. I. M. Salim, and J. Yunus, "Feasibility study of breast cancer risk monitoring using thermography technique in Malaysia," *Jurnal Teknologi*, vol. 77, no. 7, pp. 49–54, Nov. 2015, doi: 10.11113/jt.v77.6247.
[35] M. C. Araujo, R. C. F. Lima, and R. M. C. R. de Souza, "Interval symbolic feature extraction for thermography breast cancer detection," *Expert Syst. Appl.*, vol. 41, no. 15, pp. 6728–6737, Nov. 2014, doi: 10.1016/j.eswa.2014.04.027.
[36] J. P. S. de Oliveira, A. Conci, M. G. Perez, and V. H. Andaluz, "Segmentation of infrared images: A new technology for early detection of breast diseases," in *Proc. IEEE Int. Conf. Ind. Technol. (ICIT)*, Mar. 2015, pp. 1765–1771, doi: 10.1109/ICIT.2015.7125353.
[37] P. Yadav and V. Jethani, "Breast thermograms analysis for cancer detection using feature extraction and data mining technique," in *Proc. Int. Conf. Adv. Inf. Commun. Technol. Comput. (AICTC)*, 2016, pp. 1–5, doi: 10.1145/2979779.2979866.
[38] M. A. D. Santana, J. M. S. Pereira, F. L. D. Silva, N. M. D. Lima, F. N. D. Sousa, G. M. S. D. Arruda, R. D. C. F. D. Lima, W. W. A. D. Silva, and W. P. D. Santos, "Breast cancer diagnosis based on mammary thermography and extreme learning machines," *Res. Biomed. Eng.*, vol. 34, no. 1, pp. 45–53, Mar. 2018, doi: 10.1590/2446-4740.05217.
[39] S. Pramanik, D. Bhattacharjee, and M. Nasipuri, "Wavelet based thermogram analysis for breast cancer detection," in *Proc. Int. Symp. Adv. Comput. Commun. (ISACC)*, Sep. 2015, pp. 205–212, doi: 10.1109/ISACC.2015.7377343.
[40] S. Pramanik, D. Bhattacharjee, and M. Nasipuri, "Texture analysis of breast thermogram for differentiation of malignant and benign breast," in *Proc. Int. Conf. Adv. Comput., Commun. Informat. (ICACCI)*, Sep. 2016, pp. 8–14, doi: 10.1109/ICACCI.2016.7732018.
[41] L. F. Silva, A. A. S. M. D. Santos, R. S. Bravo, A. C. Silva, D. C. Muchaluat-Saade, and A. Conci, "Hybrid analysis for indicating patients with breast cancer using temperature time series," *Comput. Methods Programs Biomed.*, vol. 130, pp. 142–153, Jul. 2016, doi: 10.1016/j.cmpb.2016.03.002.
[42] M. Abdel-Nasser, A. Moreno, and D. Puig, "Breast cancer detection in thermal infrared images using representation learning and texture analysis methods," *Electronics*, vol. 8, no. 1, p. 100, Jan. 2019, doi: 10.3390/electronics8010100.
[43] M. D. F. O. Baffa and L. G. Lattari, "Convolutional neural networks for static and dynamic breast infrared imaging classification," in *Proc. 31st SIBGRAPI Conf. Graph., Patterns Images (SIBGRAPI)*, Oct. 2018, pp. 174–181, doi: 10.1109/SIBGRAPI.2018.00029.
[44] J. Zuluaga-Gomez, Z. Al Masry, K. Benaggoune, S. Meraghni, and N. Zerhouni, "A CNN-based methodology for breast cancer diagnosis using thermal images," 2019, *arXiv:1910.13757*. [Online]. Available: http://arxiv.org/abs/1910.13757
[45] U. R. Gogoi, M. K. Bhowmik, A. K. Ghosh, D. Bhattacharjee, and G. Majumdar, "Discriminative feature selection for breast abnormality detection and accurate classification of thermograms," in *Proc. Int. Conf. Innov. Electron., Signal Process. Commun. (IESC)*, Apr. 2017, pp. 39–44, doi: 10.1109/IESPC.2017.8071861.
[46] S. T. Kakileti, A. Dalmia, and G. Manjunath, "Exploring deep learning networks for tumor segmentation in infrared images," *Quantum Infr. Thermogr. J.*, vol. 17, no. 3, pp. 153–168, 2019, doi: 10.1080/17686733.2019.1619355.
[47] S. Min, J. Heo, Y. Kong, Y. Nam, P. Ley, B.-K. Jung, D. Oh, and W. Shin, "Thermal infrared image analysis for breast cancer detection," *KSII Trans. Internet Inf. Syst.*, vol. 11, no. 2, pp. 1134–1147, 2017, doi: 10.3837/tiis.2017.02.029.
[48] H. T. Iqbal, B. Majeed, U. Khan, and M. A. Bin Altaf, "An infrared high classification accuracy hand-held machine learning based breast-cancer detection system," in *Proc. IEEE Biomed. Circuits Syst. Conf. (BioCAS)*, Oct. 2019, pp. 1–4, doi: 10.1109/BIOCAS.2019.8918687.
[49] J. Ma, P. Shang, C. Lu, S. Meraghni, K. Benaggoune, J. Zuluaga, N. Zerhouni, C. Devalland, and Z. A. Masry, "A portable breast cancer detection system based on smartphone with infrared camera," *Vibroeng. Procedia*, vol. 26, no. 9, pp. 57–63, 2019, doi: 10.21595/vp.2019.20978.
[50] S. Tello-Mijares, F. Woo, and F. Flores, "Breast cancer identification via thermography image segmentation with a gradient vector flow and a convolutional neural network," *J. Healthcare Eng.*, vol. 2019, pp. 12–19, Nov. 2019.
[51] S. Guan, N. Kamona, and M. Loew, "Segmentation of thermal breast images using convolutional and deconvolutional neural networks," in *Proc. IEEE Appl. Imag. Pattern Recognit. Workshop (AIPR)*, Oct. 2018, pp. 1–6.
[52] J. C. Torres-Galvan, E. Guevara, and F. J. Gonzalez, "Comparison of deep learning architectures for pre-screening of breast cancer thermograms," in *Proc. Photon. North (PN)*, May 2019, pp. 2–3, doi: 10.1109/PN.2019.8819587.
[53] S. T. Kakileti, G. Manjunath, and H. J. Madhu, "Cascaded CNN for view independent breast segmentation in thermal images," in *Proc. 41st Annu. Int. Conf. IEEE Eng. Med. Biol. Soc. (EMBC)*, Jul. 2019, pp. 6294–6297, doi: 10.1109/embc.2019.8856628.
[54] A. Canziani, A. Paszke, and E. Culurciello, "An analysis of deep neural network models for practical applications," 2016, *arXiv:1605.07678*. [Online]. Available: http://arxiv.org/abs/1605.07678
[55] C. Szegedy, S. Ioffe, V. Vanhoucke, and A. A. Alemi, "Inception-v4, inception-resnet and the impact of residual connections on learning," in *Proc. 31st AAAI Conf. Artif. Intell. (AAAI)*, 2017, pp. 4278–4284. [Online]. Available: https://www.aaai.org
[56] U. R. Gogoi, G. Majumdar, M. K. Bhowmik, A. K. Ghosh, and D. Bhattacharjee, "Breast abnormality detection through statistical feature analysis using infrared thermograms," in *Proc. Int. Symp. Adv. Comput. Commun. (ISACC)*, Sep. 2015, pp. 258–265, doi: 10.1109/ISACC.2015.7377351.
[57] F. J. Fernández-ovies and E. J. De Andrés, "Detection of breast cancer using infrared thermography and deep neural networks detection of breast cancer using infrared thermography and deep neural networks," in *Bioinformatics and Biomedical Engineering*. Berlin, Germany: Springer-Verlag, 2019, doi: 10.1007/978-3-030-17935-9.
[58] R. Roslidar, K. Saddami, F. Arnia, M. Syukri, and K. Munadi, "A study of fine-tuning CNN models based on thermal imaging for breast cancer classification," in *Proc. IEEE Int. Conf. Cybern. Comput. Intell. (CyberneticsCom)*, Aug. 2019, pp. 77–81.

[59] S. Mambou, P. Maresova, O. Krejcar, A. Selamat, and K. Kuca, "Breast cancer detection using infrared thermal imaging and a deep learning model," *Sensors*, vol. 18, no. 9, p. 2799, Aug. 2018, doi: 10.3390/s18092799.
[60] S. Pramanik, D. Banik, D. Bhattacharjee, M. Nasipuri, M. K. Bhowmik, and G. Majumdar, "Suspicious-region segmentation from breast thermogram using DLPE-based level set method," *IEEE Trans. Med. Imag.*, vol. 38, no. 2, pp. 572–584, Feb. 2019, doi: 10.1109/TMI.2018.2867620.
[61] S. Mitra and C. Balaji, "A neural network based estimation of tumour parameters from a breast thermogram," *Int. J. Heat Mass Transf.*, vol. 53, nos. 21–22, pp. 4714–4727, Oct. 2010, doi: 10.1016/j.ijheatmasstransfer.2010.06.020.
[62] J. Koay, C. Herry, and M. Frize, "Analysis of breast thermography with an artificial neural network," in *Proc. 26th Annu. Int. Conf. IEEE Eng. Med. Biol. Soc.*, Sep. 2004, pp. 1159–1162.
[63] V. Lessa and M. Marengoni, "Applying artificial neural network for the classification of breast cancer using infrared thermographic images," in *Computer Vision and Graphics* (Lecture Notes in Computer Science), vol. 9972, L. J. Chmielewski, A. Datta, R. Kozera, and K. Wojciechowski, Eds. Cham, Switzerland: Springer, 2016.
[64] E. Y. K. Ng, S. C. Fok, Y. C. Peh, F. C. Ng, and L. S. J. Sim, "Computerized detection of breast cancer with artificial intelligence and thermograms," *J. Med. Eng. Technol.*, vol. 26, no. 4, pp. 152–157, 2002, doi: 10.1080/03091900210146941.
[65] U. R. Acharya, E. Y. K. Ng, J.-H. Tan, and S. V. Sree, "Thermography based breast cancer detection using texture features and support vector machine," *J. Med. Syst.*, vol. 36, no. 3, pp. 1503–1510, Jun. 2012, doi: 10.1007/s10916-010-9611-z.
[66] U. Raghavendra, A. Gudigar, T. N. Rao, E. J. Ciaccio, E. Y. K. Ng, and U. R. Acharya, "Computer-aided diagnosis for the identification of breast cancer using thermogram images: A comprehensive review," *Infr. Phys. Technol.*, vol. 102, Nov. 2019, Art. no. 103041, doi: 10.1016/j.infrared.2019.103041.
[67] U. Raghavendra, U. R. Acharya, E. Y. K. Ng, J.-H. Tan, and A. Gudigar, "An integrated index for breast cancer identification using histogram of oriented gradient and kernel locality preserving projection features extracted from thermograms," *Quant. Infr. Thermography J.*, vol. 13, no. 2, pp. 195–209, Jul. 2016, doi: 10.1080/17686733.2016.1176734.
[68] M. Etehadtavakol and E. Y. K. Ng, "Breast thermography as a potential non-contact method in the early detection of cancer: A review," *J. Mech. Med. Biol.*, vol. 13, no. 2, Apr. 2013, Art. no. 1330001, doi: 10.1142/S0219519413300019.
[69] A. Morales-Cervantes, E. S. Kolosovas-Machuca, E. Guevara, M. M. Reducindo, A. B. B. Hernández, M. R. García, and F. J. González, "An automated method for the evaluation of breast cancer using infrared thermography," *EXCLI J.*, vol. 17, pp. 989–998, Oct. 2018, doi: 10.17179/excli2018-1735.
[70] J. Zuluaga-Gomez, N. Zerhouni, Z. Al Masry, C. Devalland, and C. Varnier, "A survey of breast cancer screening techniques: Thermography and electrical impedance tomography," *J. Med. Eng. Technol.*, vol. 43, no. 5, pp. 305–322, Jul. 2019, doi: 10.1080/03091902.2019.1664672.
[71] A. Ghafarpour, I. Zare, H. G. Zadeh, J. Haddadnia, F. J. S. Zadeh, Z. E. Zadeh, S. Kianersi, S. Masoumzadeh, and S. Nour, "A review of the dedicated studies to breast cancer diagnosis by thermal imaging in the fields of medical and artificial intelligence sciences," *J. Biomed. Res.*, vol. 27, no. 2, pp. 543–552, 2016.
[72] S. G. Kandlikar, I. Perez-Raya, P. A. Raghupathi, J.-L. Gonzalez-Hernandez, D. Dabydeen, L. Medeiros, and P. Phatak, "Infrared imaging technology for breast cancer detection—Current status, protocols and new directions," *Int. J. Heat Mass Transf.*, vol. 108, pp. 2303–2320, May 2017, doi: 10.1016/j.ijheatmasstransfer.2017.01.086.
[73] A. Hakim and R. N. Awale, "Thermal imaging—An emerging modality for breast cancer detection: A comprehensive review," *J. Med. Syst.*, vol. 44, no. 8, pp. 1–18, Aug. 2020, doi: 10.1007/s10916-020-01581-y.
[74] R. Mulaveesala and G. Dua, "Non-invasive and non-ionizing depth resolved infra-red imaging for detection and evaluation of breast cancer: A numerical study," *Biomed. Phys. Eng. Exp.*, vol. 2, no. 5, Sep. 2016, Art. no. 055004, doi: 10.1088/2057-1976/2/5/055004.
[75] A. Sharma, G. Dua, and R. Mulaveesala, "Breast cancer detection using frequency modulated thermal wave imaging," *Imag. Sci. J.*, vol. 67, no. 7, pp. 396–406, Oct. 2019, doi: 10.1080/13682199.2019.1679442.
[76] G. Dua and R. Mulaveesala, "Applicability of active infrared thermography for screening of human breast: A numerical study," *J. Biomed. Opt.*, vol. 23, no. 3, pp. 1–9, Mar. 2018, doi: 10.1117/1.JBO.23.3.037001.
[77] S. N. Prasad and D. Houserkova, "The role of various modalities in breast imaging," *Biomed. Papers*, vol. 151, no. 2, pp. 209–218, 2007, doi: 10.5507/bp.2007.036.
[78] S. Mishra, A. Prakash, S. K. Roy, P. Sharan, and N. Mathur, "Breast cancer detection using thermal images and deep learning," in *Proc. 7th Int. Conf. Comput. for Sustain. Global Develop. (INDIACom)*, Mar. 2020, pp. 211–216.
[79] R. Roslidar, A. Rahman, R. Muharar, M. R. Syahputra, F. Arnia, M. Syukri, B. Pradhan, and K. Munadi, "A review on recent progress in thermal imaging and deep learning approaches for breast cancer detection," *IEEE Access*, vol. 8, pp. 116176–116194, 2020, doi: 10.1109/ACCESS.2020.3004056.

MOHAMMED ABDULLA SALIM AL HUSAINI is currently pursuing the Ph.D. degree with the Department of Electrical and Computer Engineering, International Islamic University Malaysia. His research interests include image processing, signal processing, and AI applications.

MOHAMED HADI HABAEBI (Senior Member, IEEE) is currently a Professor with the Department of Electrical and Computer Engineering, International Islamic University Malaysia (IIUM). His research interests include the IoT, mobile app development, networking, blockchain, AI applications in image processing, cyber-physical security, wireless communications, small antenna, and channel propagation modeling.

SHIHAB A. HAMEED (Senior Member, IEEE) is currently a Professor with the Department of Computer Science, Cihan University-Ebril, Iraq. His research interests include software engineering and quality, healthcare and medical applications, multimedia and mobile apps, professional ethics, green ICT, and e-waste.

MD. RAFIQUL ISLAM (Senior Member, IEEE) is currently a Professor with the Department of Electrical and Computer Engineering, International Islamic University Malaysia (IIUM). His research interests include the IoT applications, radio link design, RF propagation measurement and RF design, smart antennas, and array antennas design.

TEDDY SURYA GUNAWAN (Member, IEEE) is currently a Professor with the Department of Electrical and Computer Engineering, International Islamic University Malaysia. His research interests include speech and audio processing, biomedical signal processing and instrumentation, image and video processing, and parallel computing.